Effects of WD-3 on tumor growth and the expression of integrin $\alpha_v\beta_3$ and ERK1/2 in mice bearing human gastric cancer using the ^{18}F-RGD PET/CT imaging system

CHUNHUI JIN[1*], BAO-NAN ZHANG[1*], ZHIPENG WEI[1], BO MA[2], QI PAN[3] and PINGPING HU[1]

[1]Department of Oncology, Wuxi Hospital of Traditional Chinese Medicine, Wuxi, Jiangsu 214000;
[2]Department of Surgery, Affiliated Central Hospital of Huzhou Teachers College, Huzhou, Zhejiang 313000;
[3]Department of Oncology, The Second Wuxi Hospital of Traditional Chinese Medicine, Wuxi, Jiangsu 214000, P.R. China

Received March 29, 2016; Accepted March 16, 2017

DOI: 10.3892/mmr.2017.7827

Abstract. Activation of the vitronectin receptor $\alpha_v\beta_3$ and the phosphorylation of extracellular signal-regulated kinase (ERK)1/2 are critical events during tumor development and progression. The aim of the present study was to investigate the effects of WD-3, a formula used in traditional Chinese medicine, on integrin $\alpha_v\beta_3$ and ERK1/2 expression *in vivo* using a nude mouse-human gastric cancer xenograft model combined with non-invasive, real-time ^{18}F-Arg-Gly-Asp (RGD) positron emission tomography (PET)/computerized tomography (CT) imaging methods. SGC-7901 human gastric cancer cells were subcutaneously injected into BALB/c nude mice. Following tumor development, animals were randomly assigned into the following 4 groups (n=6 mice/group): Control group (CG), Chinese medicine group (CMG), Western medicine group (WMG) and Chinese and Western medicine combination group (CMG + WMG). Mice in the CG and CMG received daily intragastric injections of 0.5 ml saline and 0.5 ml WD-3, respectively. Mice in the WMG received an intravenous injection of albumin-bound paclitaxel (25 mg/kg) on days 0, 2 and 4 Mice in the CMG + WMG received combination therapy of WD-3 and albumin-bound paclitaxel. Tumor growth was monitored using standard caliper technique and via PET imaging. ^{18}F-RGD PET/CT analysis was performed on days 3, 7, 18 and 24 following drug administration. Radioactivity uptake was measured and expressed as the percentage of injected dose (ID) per tissue weight (%ID/g) and the standardized uptake value (SUV). Animals were sacrificed at 30 days following treatment and tumor weight was measured. Immunohistochemistry was used to detect the expression of phosphorylated (p)-ERK1/2 protein in tumor tissue samples. No statistically significant differences were observed in %ID/g and SUV among the various groups prior to treatment. At the end of treatment, mice in the CMG, WMG and CMG + WMG exhibited significantly reduced tumor mass when compared with mice in the CG. In addition, mice in the CMG and CMG + WMG demonstrated reduced %ID/g and SUV when compared with mice in the CG. Conversely, mice in the WMG exhibited no significant difference in %ID/g and SUV compared with the CG. Furthermore, p-ERK1/2 expression was significantly reduced in mice from all treatment groups when compared with those in the CG. The results of the present study suggest that the traditional Chinese formula WD-3 may inhibit gastric tumor growth, potentially via the downregulation of integrin $\alpha_v\beta_3$ and the inhibition of ERK1/2 phosphorylation *in vivo*.

Correspondence to: Dr Pingping Hu, Department of Oncology, Wuxi Hospital of Traditional Chinese Medicine, 8 Zhongnan West Road, Wuxi, Jiangsu 214000, P.R. China
E-mail: pingpinghoo@126.com

*Contributed equally

Abbreviations: ERK, extracellular signal-regulated kinase; RGD, Arg-Gly-Asp; PET, positron emission tomography; CT, computerized tomography; SUV, standardized uptake value; FAK, focal adhesion kinase; MMP, matrix metalloproteinase

Key words: WD-3 agent, traditional Chinese medicine compound, gastric carcinoma, positron emission tomography, integrin $\alpha_v\beta_3$, extracellular signal regulated kinase 1/2

Introduction

Gastric carcinoma is one of the most common gastrointestinal malignancies worldwide. Gastric cancer has been reported as the fourth leading cause of cancer-associated morbidity and the third most common cause of cancer-associated mortality worldwide in 2012, as it accounts for 8.8% of all cancer death cases (1). Eastern Asia, including Japan, Korea and China, is a geographical region with one of the highest incidence rates of gastric cancer, accounting for ~2/3 gastric cancer cases worldwide (2).

Integrins are a group of transmembrane receptors that mediate adhesion between cells and components of the extracellular matrix. Integrins have been reported to interact with focal adhesion kinase (FAK), leading to the activation of p130Crk-associated substrate and paxillin-mediated signaling pathways to modulate the expression of the

extracellular signal-regulated kinase (ERK) gene. This leads to modulation of tumor angiogenesis, invasion, metastasis and apoptosis (3-5). In addition, integrins have been demonstrated to be highly expressed in several types of malignant tumors, including gastric and squamous cell carcinoma, and melanoma (6,7). The ERK intracellular signal transduction pathway has been implicated in numerous cellular processes. The ERK signaling cascade communicates extracellular signals from surface receptors to the cell nucleus; a process which has been reported to regulate various cellular functions, including cell growth, development, differentiation, division and death (8,9). Phosphorylated (p)-ERK is the active form of ERK (10). ERK has been demonstrated to inhibit apoptosis through activation of p90 ribosomal s6 kinase (11,12). In addition, p-ERK promotes cellular proliferation by activating various transcription factors, including CCAAT-enhancer-binding protein, Elk-1, c-Jun, c-Myc and c-Fos, which promote cell cycle progression from the G_1 to the S phase, thereby facilitating malignant tumor growth (13). Furthermore, the activation of ERK1/2 has been reported to enhance the protein expression of matrix metalloproteinase (MMP)-2 and MMP-9, which degrade the basement membrane barrier (14), and thus enhance epithelial-to-mesenchymal transition to promote tumor cell invasion and metastasis (15).

Positron emission tomography (PET) is one of the most common non-invasive molecular imaging methods that is used to observe tumor development *in vivo*, through the observation of metabolic activity. Small animal PET scans (MicroPET) have been designed to study human diseases using *in vivo* experimental animal models (16). MicroPET allows continuous longitudinal monitoring of the same animal, and the collection of data in real-time. In addition, it may be used for the non-invasive, dynamic and quantitative observation of physiological and pathological alterations *in vivo*, thus facilitating the study of disease pathogenesis and the evaluation of drug efficacy (17,18). The ^{18}F-labeled Arg-Gly-Asp (RGD) peptide has been demonstrated to specifically target the vitronectin receptor $\alpha_v\beta_3$, a member of the integrin superfamily (19). Targeting the vitronectin $\alpha_v\beta_3$ integrin receptor could be used as a tool to visualize and quantify integrin $\alpha_v\beta_3$ expression levels, thus facilitating observation of the distribution of integrin $\alpha_v\beta_3$ in the body using MicroPET.

WD-3 also known as Weitiao No. 3 is a formula developed by Professor Jingfang Zhao in 1997 (20). Previous studies have suggested that treatment with WD-3 may improve the quality of life in patients with advanced colon cancer and gastric carcinoma. Among patients with advanced gastric cancer receiving treatment with WD-3, the disease control rate (88.16%) and the 3-year overall survival rate (61.18%) were significantly improved when compared with untreated patients (20,21). However, the molecular mechanisms underlying the inhibitory effects of WD-3 on tumor cells have yet to be elucidated. The present study aimed to investigate the putative effects of WD-3 on vitronectin receptor $\alpha_v\beta_3$ in a nude mouse-human gastric cancer xenograft model using ^{18}F-RGD PET/computerized tomography (CT). Immunohistochemistry was performed to examine the effects of WD-3 administration on p-ERK1/2 protein expression, and thus the implication of the integrin $\alpha_v\beta_3$/FAK/mitogen-activated protein kinase/ERK signaling pathway in the mechanism of action of WD-3.

Materials and methods

Tumor cell line and animals. A total of 24 male BALB/c nude mice (age, 6 weeks; weight, 18-24 g) were purchased from Shanghai SLAC Laboratory Animal Co., Ltd. [Shanghai, China; certificate no. SCXK (Shanghai) 2012-0002] and maintained in a specific pathogen-free animal facility. They were housed with free access to water and food in a specific pathogen-free facility under a 12-h light/dark cycle at 50±10% humidity and 21±2˚C. The SGC-7901 human gastric cancer cell line was purchased from the Chinese Academy of Sciences Cell Bank.

The experimental protocols used in the present study were approved by the Ethics Committee of the Jiangsu Institute of Nuclear Medicine (Wuxi, China). Ether was used for mouse anesthesia and euthanasia.

Experimental drugs and reagents. WD-3 was composed of 10 g *Condonopsis pilosula* root, 10 g *Atractylodes macrocephalae*, 10 g *Wolfiporia extensa*, 10 g P*olyporus umbrellatus*, 10 g oryzae germinatus, fructus, 10 g wheat germ, 6 g *Pinellia ternata,* 6 g *Citrus tangerina*-Peel, 30 g *Semen coicis,* 10 g *Dioscorea polystachya*, 10 g poria with hostwood, 10 g *Eriobotrya japonica* leaf and 3 g *radix liquiritiae*. Raw herbs were provided by the Traditional Medicine Pharmacy of the Wuxi Traditional Chinese Medicine Hospital (Wuxi, China). Herbs were placed into a decocting pot with a 5-fold volume of water and soaked for 30 min. The mixture was boiled over a strong flame before herbs were decocted over a reduced flame for 30 min and filtered. Any residue was decocted continuously for 30 min with a 5-fold volume of water and filtered. Filtrates were combined and concentrated into a crude drug solution with a concentration of 2.85 g/ml and refrigerated at 2-8˚C. Albumin-bound paclitaxel (100 mg aliquots for injection) was purchased from Abraxis BioScience, Inc. (Los Angeles, CA, USA).

Herbs were placed into a decocting pot with a 5-fold volume of water and soaked for 30 min. The mixture was boiled over a strong flame before herbs were decocted over a reduced flame for 30 min and filtered. Any residue was decocted continuously for 30 min with a 5-fold volume of water and filtered. Filtrates were combined and concentrated into a crude drug solution with a concentration of 2.85 g/ml and refrigerated at 2-8˚C.

Tumor xenografts in nude mice. SGC-7901 human gastric cancer cells were conventionally cultured (RPMI-1640 nutrient solution containing 100 IU/ml penicillin and 100 μg/ml streptomycin (HyClone Laboratories, Inc., Logan, UT, USA), cultivated with 5% CO_2 at 37˚C), and the cell concentration was adjusted to $1x10^7$ cells/ml and cells were resuspended in phosphate-buffered saline. Under aseptic conditions, SGC-7901 cells (~$2x10^6$ cells/mouse) were implanted subcutaneously into the right forelimb of nude BALB/c mice. After 7 days, tumors that grew to a measurable size with a tumor diameter of ~0.5 cm were selected to establish the transplanted tumor model, and were randomly assigned into the following 4 groups (n=6 mice/group): Control group (CG), Chinese medicine group (CMG), Western medicine group (WMG) and Chinese and Western medicine combination group (WMG + CMG). Mice in the CG received daily intragastric injections of 0.5 ml saline; mice in the CMG received daily intragastric

injections of 0.5 ml WD-3 (containing 2.85 g/ml crude drug); mice in the WMG + CMG received daily intragastric injections of 0.5 ml WD-3, and intravenously administered with albumin-bound paclitaxel (25 mg/kg) via the tail vein on days 0, 2 and 4; mice in the WMG received intravenous injections of albumin-bound paclitaxel (25 mg/kg) on days 0, 2 and 4. The duration of treatment was 30 days.

Tumor assessment. Tumor growth was assessed using standard caliper measurement twice a week for 4 weeks. The following formula was used to calculate tumor volume: Tumor volume (mm^3)=(tumor length x width x height)/2, with all measurements in mm. Following 30 days of treatment, mice were sacrificed and tumor xenografts were harvested. The rate of tumor growth inhibition was calculated following the evaluation of tumor weight, according to the following formula: Tumor inhibition rate (%)=[(tumor weight (g) in the control group-tumor weight (g) in treatment group)/tumor weight (g) in the control group] x100.

MicroPET was used to assess tumor growth. ^{18}F-RGD PET scans were performed prior to the initiation of drug treatment (day 0) and at 3, 7, 18 and 24 days post-drug administration. The MicroPET protocol was as follows: 1 h prior to scanning, a single tracer ^{18}F-RGD injection of 100±20 μCi (100-200 μl; Jiangsu Institute of Nuclear Medicine, Jiangsu, China) was intravenously administered via the lateral tail vein. Mice were not required to fast and were administered with drugs while conscious. Normal eating continued following drug administration. A total of 1 h following administration, 10-min static MicroPET was performed. PET scans and image analysis were performed using an Inveonmicro PET (Siemens Healthineers, Erlangen, Germany).

MicroPET data processing. Scans were reconstructed using Inveon Acquisition Workplace software (version 1.4; Siemens Healthineers), using a three-dimensional ordered-subset expectation maximization/maximum a posteriori algorithm with the following parameters: matrix, 128x128x159; pixel size, 0.86x0.86x0.8 mm, and β-value, 1.5, with uniform resolution. Acquisition time, 10 min; acquisition energy window, 350-650 keV. The Micro PET Analysis software (version ASI Pro 6.7.1.1; Siemens AG, Munich, Germany) was used to outline the brain, heart, liver, kidney and tumor tissue as the regions of interest (ROIS). The mean uptake value of radioactive material (PET units/g) of the region of interest was obtained. The radioactivity concentration (accumulation) within a tumor or an organ was obtained from mean pixel values within the multiple ROI volume, which had been converted to MBq/ml/min using a conversion factor. The conversion to MBq/g/min assumed a tissue density of 1 g/ml. Imaging ROI-derived %ID/g was calculated by dividing the ROIs by the administered activity injected dose per gram.

p-ERK1/2 protein expression. Following 30 days of treatment, mice were sacrificed, and tumor tissue samples were harvested and fixed in 4% paraformaldehyde for 24 h at 25˚C. Immunohistochemistry was used to detect the expression of p-ERK1/2 protein. Tissue sections (4-μm) were prepared from 10% formalin-fixed (for 24 h at 25˚C) and paraffin-embedded tissues. Following deparaffinization and rehydration with ethanol (70-100%), the slides were heated to 100˚C in 10 mmol/l sodium citrate buffer (pH, 6) for 15 min to for antigen retrieval. Endogenous peroxidase activity was blocked by incubating at 25˚C with 0.6% H_2O_2 in methanol for 20 min. Sections were subsequently blocked with 10% normal horse serum (Wuhan Boster Biological Technology, Ltd., Wuhan, China) for 5 min at 25˚C. Following blocking, sections were incubated with the Rabbit monoclonal anti-p-ERK1 and p-ERK2 (1:1,000; cat. no. sc-20147; Santa Cruz Biotechnology, Inc.), Sections were incubated with primary antibodies at room temperature for 2 h. The slides were incubated with streptavidin-horseradish peroxidase conjugated biotinylated secondary antibodies Biotin Goat Anti-Rabbit immunoglobulin G (IgG; 1:2,000; cat. no. K4009; Dako; Agilent Technologies, Inc.) for 30 min at room temperature. Following incubation, an avidin/strepavidin complex (Dako; Agilent Technologies, Inc.) was added. A non-specific staining blocker (GeneTex Biotechnology Co., Ltd., Shanghai, China) and enzyme-labeled sheep anti-rabbit IgG polymer reagent (GeneTex Biotechnology Co., Ltd.,) were added according to the manufacturer's protocol. The antigen detection was conducted via a color reaction with 3,3'-diaminobenzidine (Dako; Agilent Technologies, Inc.). Sections were counterstained using hematoxylin (AppliChem Inc., St Louis, MO, USA) and mounted with Aquatex (Merck KGaA, Darmstadt, Germany). Stained samples were observed under a light microscope. p-ERK1/2 staining was yellow, brown or tan in color, primarily localized to the nucleus and partly in the cytoplasm. For each tissue section, a total of 4 fields of view were analyzed under an inverted microscope at x400 magnification, and 1,500 cells were randomly chosen to counted by 2 independent blinded investigators (authors 1 and 2) to calculate the percentage of p-ERK1/2-positive cells by IPP software (Image-Pro Plus version 6.0, Media Cybernetics, Inc., Rockville, MD, USA) and the results were consistent between the two readings. As previously described by Watanabe *et al* (22), the immunohistochemical semi-quantitative scoring criteria that were used were as follows: <5% positive cells, negative (0 points); 5-20% positive cells, weakly positive (1 point); 20-50% positive cells, positive (2 points); 50-75% positive cells, strong positive (3 points); >75% positive cells, very strong positive (4 points). Color intensity scoring criteria were as follows: No color, 0 points; light color, 1 point; medium color, 2 points; darker color, 3 points; deep color, 4 points. The overall rating was calculated according to the following formula: Overall rating=(positive cell percentage score x color intensity score)/4. A high overall rating suggested that p-ERK1/2 protein expression was high, whereas a low overall rating suggested low p-ERK1/2 protein expression.

Statistical analysis. Statistical analysis of differences among groups was assessed by one-way analysis of variance followed by a post hoc least significant difference (equal variances) or Tamhane's T2 test (unequal variances) for multiple comparisons. Statistical analysis was performed using SPSS software (version 15.0; SPSS, Inc., Chicago, IL, USA). The measurement data were presented as the mean ± standard deviation of three independent experiments (n=6 per group). $P<0.05$ was considered to indicate a statistically significant difference.

Results

Effects of WD-3 on gastric tumor volume in vivo. During the initial 10 days following the initiation of drug treatment, mice in the WMG and CMG + WMG exhibited a decrease in tumor volume; however, from day 10 onwards, tumor volumes followed an increasing trend (Fig. 1). Notably, mice in the CMG exhibited tumor growth rates similar to mice in the CG for the initial 10 days of treatment; however, from day 15 onwards, tumor growth in the CMG appeared to slow when compared with the CG (Fig. 1).

Effects of WD-3 on gastric tumor weight in vivo. Following 30 days of treatment, tumors were collected and weighed. The results demonstrated that tumor weight in the CMG, WMG and CMG + WMG was significantly reduced (P<0.05) when compared with in the CG (Table I). In addition, no statistically significant difference in tumor weight was detected among mice in the CMG, WMG and CMG + WMG (Table I).

^{18}F-RGD PET/CT results. The results of the PET/CT scans indicated increased uptake of radioactive material was observed at days 3, 7, 18 and 24 in the CG when compared with day 0 (Figs. 2 and 3). In the WMG, %ID/g values decreased on days 3 and 7 of treatment, and on day 3 the %ID/g value was significantly lower when compared with the CG (P<0.05; Fig. 2). However, on days 18 and 24 of treatment radioactivity uptake was increased in mice in the WMG when compared with 3 and 7 days. In addition, mice in the CMG + WMG demonstrated significantly decreased radioactivity uptake on treatment days 3, 18 and 24 compared with mice in the CG (Fig. 2). As treatment progressed, radioactivity uptake in CMG mice gradually decreased; notably mice in the CMG exhibited significantly decreased %ID/g values on days 18 and 24 when compared with mice in the CG (Figs. 2 and 3).

Effects of WD-3 on p-ERK1/2 protein expression levels in tumor tissue samples. p-ERK1/2 proteins are primarily expressed in the nucleus (23). In the present study, immunohistochemical examination and semi-quantification suggested that mice in the CMG, WMG and CMG + WMG exhibited significantly reduced p-ERK1/2 protein expression, indicated by weak p-ERK staining and significantly lower comprehensive scores when compared with mice in the CG (Fig. 4; Table II).

Table I. Tumor weight and rate of growth inhibition.

Group	Tumor weight (g)	Tumor inhibition rate (%)
CG	0.83±0.20	-
CMG	0.72±0.26[a]	12.97±1.21
WMG	0.58±0.41[a]	30.61±2.52
WMG + CMG	0.56±0.23[a]	32.71±1.43

[a]P<0.05 vs. the CG. Data are expressed as the mean ± standard deviation of three independent experiments (n=6 per group). CG, control group mice treated with saline; WMG, Western medicine group mice treated with albumin-bound paclitaxel; CMG, Chinese medicine group mice treated with WD-3; CMG + WMG, mice were treated with a combination of albumin-bound paclitaxel and WD-3.

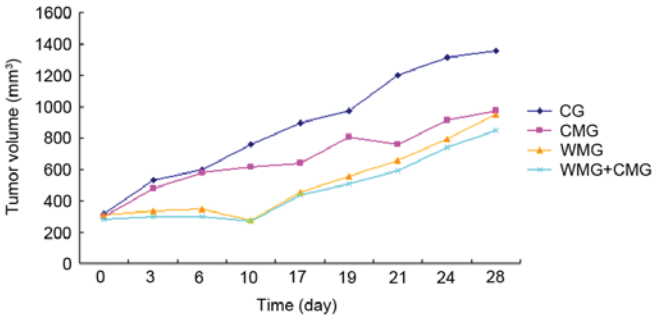

Figure 1. Tumor volumes (mm^3) in nude mice with SGC-7901 human gastric tumor xenografts were evaluated over the course of the 30-day treatment with saline, WD-3 and/or albumin-bound paclitaxel. Data are expressed as the mean ± standard deviation of three independent experiments (n=6 per group). CG, control group mice treated with saline; WMG, Western medicine group mice treated with albumin-bound paclitaxel; CMG, Chinese medicine group mice treated with WD-3; CMG + WMG, mice were treated with a combination of albumin-bound paclitaxel and WD-3.

Discussion

Clinical studies have reported that albumin-bound paclitaxel inhibit gastric cancer development in humans (24). The present study demonstrated that nude mice bearing human gastric tumor xenografts treated with albumin-bound paclitaxel (WMG), as well as with a combination of albumin-bound paclitaxel and WD-3 (CMG + WMG) exhibited significantly reduced gastric tumor mass when compared with control mice, thus confirming the antitumor efficacy of paclitaxel. A previous study demonstrated that gastric cancer cells could be characterized by high integrin $\alpha_v\beta_3$ expression, which suggests that this factor may be a potential biomarker for the evaluation of tumor prognosis in patients with gastric cancer (25). The ^{18}F-RGD PET results revealed that radioactivity SUVs were decreased during the early stages of treatment in xenografted mice in the WMG and CMG + WMG groups. In addition, the results of the present study suggest that paclitaxel may inhibit tumor angiogenesis via downregulation of integrin $\alpha_v\beta_3$ expression, thereby inhibiting tumor growth. Nevertheless, in the groups that weren't treated with albumin-bound paclitaxel the inhibition of integrin $\alpha_v\beta_3$ decreased and SUV values increased. WD-3 administration exerted no significant effects on tumor volume when compared with the CG at the beginning of treatment, conversely, tumor weight was significantly reduced in mice in the CMG when compared with those of the CG at last. In addition, ^{18}F-RGD PET revealed that on day 18 and 24 of treatment, SUVs in CMG mice were significantly decreased when compared with CG mice. These results suggested that WD-3 may inhibit tumor angiogenesis and consequently tumor growth; however, its inhibition of tumor volume's effects were less pronounced when compared with conventional chemotherapy in the early stages of treatment (days 3 and 7). However, taking into consideration the reduced toxicity associated with traditional Chinese medicine compared with antineoplastic drugs, WD-3 may have potential as an alternative therapeutic strategy for the long-term treatment of patients with cancer (21).

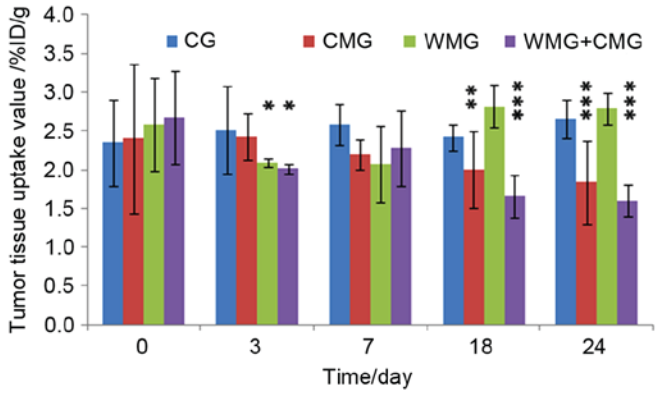

Figure 2. Radioactivity uptake was measured on days 0, 3, 7, 18 and 24 of treatment using ^{18}F-Arg-Gly-Asp positron emission tomography/computerized tomography, and expressed as the %ID/g. Data are expressed as the mean ± standard deviation of three independent experiments (n=6 per group). *P<0.05, **P<0.01, ***P<0.001 vs. the CG. CG, control group mice treated with saline; WMG, Western medicine group mice treated with albumin-bound paclitaxel; CMG, Chinese medicine group mice treated with WD-3; CMG + WMG, mice were treated with a combination of albumin-bound paclitaxel and WD-3; %ID/g, percentage of injected dose per tissue weight.

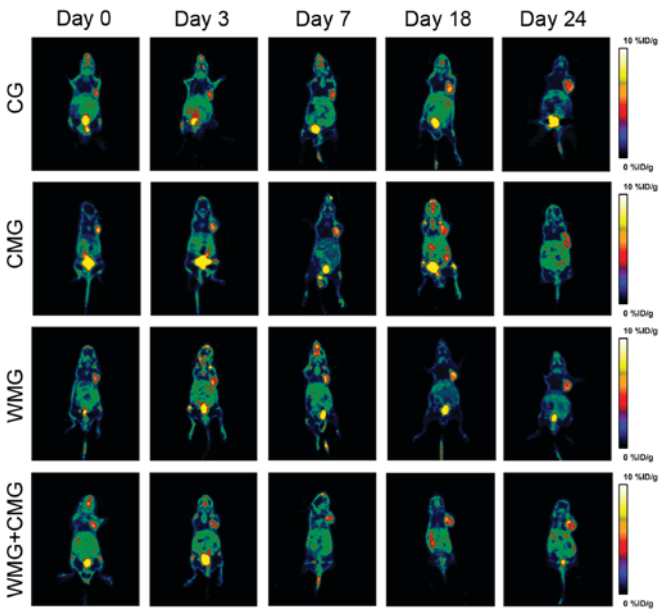

Figure 3. Coronal scans of mice on days 0, 3, 7, 18 and 24 of treatment were obtained using ^{18}F-Arg-Gly-Asp positron emission tomography/computerized tomography. CG, control group mice treated with saline; WMG, Western medicine group mice treated with albumin-bound paclitaxel; CMG, Chinese medicine group mice treated with WD-3; CMG + WMG, mice were treated with a combination of albumin-bound paclitaxel and WD-3.

The present study demonstrated that mice in the CMG + WMG displayed increased energy and average body weights when compared with mice in the WMG (data not shown). These results suggested that WD-3 may be associated with fewer toxic adverse events compared with chemotherapeutic agents.

The present study demonstrated that paclitaxel administered in combination with WD-3 effectively inhibited integrin $\alpha_v\beta_3$ expression and tumor growth, which suggests that the traditional Chinese formula WD-3 may potentially enhance the efficacy of chemotherapeutic agents when used as adjuvant treatment.

Table II. Comprehensive scores of immunohistochemical analysis of p-ERK1/2 protein expression.

	Score	
Group (n=6 mice/group)	p-ERK1	p-ERK2
CG	3.33±0.52	3.50±0.56
CMG	2.55±0.84[a]	2.67±0.82[a]
WMG	2.33±0.52[a]	2.50±0.55[a]
WMG + CMG	2.00±0.26[a]	2.17±0.41[a]

[a]P<0.05 vs. the CG. Data are expressed as the mean ± standard deviation of three independent experiments (n=6 per group). p-ERK, phosphorylated extracellular signal-regulated kinase; CG, control group mice treated with saline; WMG, Western medicine group mice treated with albumin-bound paclitaxel; CMG, Chinese medicine group mice treated with WD-3; CMG + WMG, mice were treated with a combination of albumin-bound paclitaxel and WD-3.

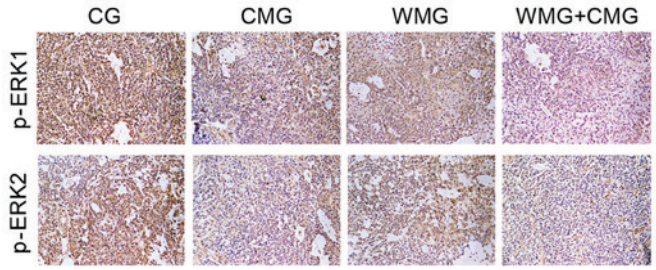

Figure 4. Immunohistochemistry was used to evaluate the protein expression levels of p-ERK1 and p-ERK2 in tumor tissue samples. Photomicrographs were captured under x100 magnification. p-ERK1/2 staining was yellow, brown or tan in color and primarily localized to the nucleus and partly in the cytoplasm. p-ERK, phosphorylated extracellular signal-regulated kinase; CG, control group mice treated with saline; WMG, Western medicine group mice treated with albumin-bound paclitaxel; CMG, Chinese medicine group mice treated with WD-3; CMG + WMG, mice were treated with a combination of albumin-bound paclitaxel and WD-3.

Immunohistochemistry demonstrated that mice in the CMG and the WMG + CMG were characterized by reduced p-ERK1/2 expression when compared with the CG. These results suggested that WD-3 may interfere with the FAK/MAPK/ERK signaling pathway through the downregulation of integrin $\alpha_v\beta_3$ expression, ultimately inhibiting ERK phosphorylation and subsequent tumor growth. However, the exact molecular mechanisms underlying the effects of WD-3 observed in the present study remain unclear. Integrin receptors have been reported to induce kinase activation and initiate downstream signal transduction cascades following mechanical stimulation (26). Further studies are required to investigate whether WD-3 may be able to interfere with FAK phosphorylation through mechanotransduction pathways, and thus inhibit tumor growth.

In conclusion, the results of the present study suggest that the traditional Chinese medicine agent, WD-3, may inhibit tumor angiogenesis by decreasing the expression of receptor $\alpha_v\beta_3$ *in vivo*, and may have potential as an adjuvant agent to be used in combination with chemotherapy for the treatment of patients with gastric cancer. In addition, WD-3 was revealed

to inhibit the gastric cancer cell growth potentially via inhibition of ERK1/2 phosphorylation. Furthermore, PET/CT scan results suggested that WD-3 may inhibit tumor angiogenesis in mice bearing human gastric cancer xenografts *in vivo*.

Acknowledgements

The present study was supported by the Science and Technology Development Foundation of Wuxi City (grant no. 0302-B010507-130006-PB).

References

1. Ferlay J, Soerjomataram I, Dikshit R, Eser S, Mathers C, Rebelo M, Parkin DM, Forman D and Bray F: Cancer incidence and mortality worldwide: Sources, methods and major patterns in GLOBCAN 2012. Int J Cancer 136: E359-E386, 2015.
2. Jemal A, Siegel R, Ward E, Murray T, Xu J and Thun MJ: Cancer statistics, 2007. CA Cancer J Clin 57: 43-66, 2007.
3. Guan JL: Integrin signaling through FAK in the regulation of mammary stem cells and breast cancer. IUBMB Life 62: 268-276, 2010.
4. Yun SP, Ryu JM and Han HJ: Involvement of β1-integrin via PIP complex and FAK/paxillin in dexamethasone-induced human mesenchymal stem cells migration. J Cell Physiol 226: 683-692, 2011.
5. Li D, Ding J, Wang X, Wang C and Wu T: Fibronectin promotes tyrosine phosphorylation of paxillin and cell invasiveness in the gastric cancer cell line AGS. Tumori 95: 769-779, 2009.
6. Missan DS, Mitchell K, Subbaram S and DiPersio CM: Integrin α3β1 signaling through MEK/ERK determines alternative polyadenylation of the MMP-9 mRNA transcript in immortalized mouse keratinocytes. PLoS One 10: e0119539, 2015.
7. Pickarski M, Gleason A, Bednar B and Duong LT: Orally active αvβ3 integrin inhibitor MK-0429 reduces melanoma metastasis. Oncol Rep 33: 2737-2745, 2015.
8. Osório-Costa F, Rocha GZ, Dias MM and Carvalheira JB: Epidemiological and molecular mechanisms aspects linking obesity and cancer. Arq Bras Endocrinol Metabol 53: 213-226, 2009.
9. O'Neil E and Kolch W: Conferring apccificity on the ubiquitous Ras/MEK signaling pathway. Br J Cancer 90: 283-288, 2004.
10. Steelman LS, Abrams SL, Whelan J, Bertrand FE, Ludwig DE, Bäsecke J, Libra M, Stivala F, Milella M, Tafuri A, *et al*: Contributions of the Raf/MEK/ERK, PI3K/PTEN/Akt/mTOR and Jak/STAT pathways to leukemia. Leukemia 22: 686-707, 2008.
11. Cheung KL, Lee JH, Shu L, Kim JH, Sacks DB and Kong AN: The Ras GTPase-activating-like protein IQGAPI mediates Nrf2 protein activation via the mitogen-activated protein kinase/extracellular signal regulated kinase (ERK) kinase (MEK)-ERK pathway. J Biol Chem 288: 22378-22386, 2013.
12. Bai Y, Cui W, Xin Y, Miao X, Barati MT, Zhang C, Chen Q, Tan Y, Cui T, Zheng Y and Cai L: Prevention by sulforaphane of diabetic cardiomyopathy is associated with up-regulation of Nrf2 expression transcription activation. J Mol Cell Cardiol 57: 82-95, 2013.
13. Muslin AJ: MAPK signalling in cardiovascular health and disease: Molecular mechanisms and therapeutic targets. Clin Sci (Lond) 115: 203-218, 2008.
14. Guruvayoorappan C and Kuttan G: Amentoflavone inhibits experimental tumor metastasis through a regulatory mechanism involving MMP-2, MMP-9, prolyl hydroxylase, lysyl oxidase, VEGF, ERK-1, ERK-2, STAT-1, nm23 and cytokines in lung tissues of C57BL/6 mice. Immunopharmacol Immunotoxicol 30: 711-727, 2008.
15. Wang J, Kuiatse I, Lee AV, Pan J, Giuliano A and Cui X: Sustained c-Jun-NH2-kinase activity promotes epithelial mesenchymal transition, invasion, and survival of breast cancer cells by regulating extracellular signal-regulated kinase activation. Mol Cancer Res 8: 266-277, 2010.
16. Chatziioannou AF: PET scanners dedicated to molecular imaging of small animal models. Mol Imaging Biol 4: 47-63, 2002.
17. Kosugi C, Saito N, Murakami K, Ochiai A, Koda K, Ono M, Sugito M, Ito M, Oda K, Seike K and Miyazaki M: Positron emission tomography for preoperative staging in patients with locally advanced or metastatic colorectal adenocarcinoma in lymphnode metastasis. Hepatogastroentero logy 55: 398-402, 2008.
18. Nahas CS, Akhurst T, Yeung H, Leibold T, Riedel E, Markowitz AJ, Minsky BD, Paty PB, Weiser MR, Temple LK, *et al*: Positron emission tomography detection of distant metastatic or synchronous disease in patients with locally advanced rectal cancer receiving preoperative chemoradiation. Ann Surg Oncol 15: 704-711, 2008.
19. Meerovitch K, Bergeron F, Leblond L, Grouix B, Poirier C, Bubenik M, Chan L, Gourdeau H, Bowlin T and Attardo G: A novel RGD antagonist that targets both alphavbeta3 and alpha-5beta1 induces apoptosis of angiogenic endothelial cells on type I collagen. Vascul Pharmacol 40: 77-89, 2003.
20. Jianliang You, Liuyong Zhou and Ming Xu: Clinical research of the treatment of advanced gastric cancer using Chinese herbal medicine WD-3. Hubei J Traditional Chinese Med 26: 8-9, 2004.
21. Zhou LY, Shan ZZ and You JL: Clinical observation on treatment of colonic cancer with combined treatment of chemotherapy and chinese herbal medicine. Chin J Integr Med 15: 107-111, 2009.
22. Watanabe H, Kanzaki H, Narukawa S, Inoue T, Katsuragawa H, Kaneko Y and Mori T: Bcl 2 and Fas expression in eutopic and ectopic human endometrium during the menstrual cycle in relation to endometrial cell apoptosis. Am J Obstet Gynecol 176: 360-368, 1997.
23. Zehorai E, Yao Z, Plotnikov A and Seger R: The subcellular localization of MEK and ERK-a novel nuclear translocation signal (NTS) paves a way to the nucleus. Mol Cell Endocrinol 314: 213-220, 2010.
24. Sasaki Y, Nishina T, Yasui H, Goto M, Muro K, Tsuji A, Koizumi W, Toh Y, Hara T and Miyata Y: Phase II trial of nanoparticle albumin-bound paclitaxel as second-line chemotherapy for unresectable or recurrent gastric cancer. Cancer Sci 105: 812-817, 2014.
25. Böger C, Warneke VS, Behrens HM, Kalthoff H, Goodman SL, Becker T and Röcken C: Integrins αvβ3 and αvβ5 as prognostic, diagnostic, and therapeutic targets in gastric cancer. Gastric Cancer 18: 784-795, 2015.
26. Friedland JC, Lee MH and Boettiger D: Mechanically activated integrin switch controls alpha5beta1 function. Science 323: 642-644, 2009.